Noguchi, C. T. (1984) *Biophys. J. 45*, 1153–1158.
Noguchi, C. T., Torchia, D. A., & Schechter, A. N. (1980) *Proc. Natl. Acad. Sci. U.S.A. 77*, 5487–5491.
Ohnishi, S., Boeyens, J. C. A., & McConnell, H. M. (1966) *Proc. Natl. Acad. Sci. U.S.A. 56*, 809–813.
Padlan, E. A., & Love, W. E. (1985) *J. Biol. Chem. 260*, 8280–8291.
Poillon, W. N., & Bertles, J. F. (1979) *J. Biol. Chem. 259*, 3462–3467.
Potel, M. J., Wellems, T. E., Vassar, R. J., Deer, B., & Josephs, R. (1984) *J. Mol. Biol. 177*, 819–839.
Rosen, L. S., & Magdoff-Fairchild, B. (1985) *J. Mol. Biol. 183*, 565–574.
Ross, P. D., Hofrichter, J., & Eaton, W. A. (1977) *J. Mol. Biol. 115*, 111–134.
Sutherland, J. W. H., Egan, W., Schechter, A. N., & Torchia, D. A. (1979) *Biochemistry 18*, 1797–1803.
Thiyagarajan, P., & Johnson, M. E. (1983) *Biophys. J. 42*, 269–274.
Thomas, D. D., Dalton, L. R., & Hyde, J. S. (1976) *J. Chem. Phys. 65*, 3006–3024.
Wellems, T. E., & Josephs, R. (1979) *J. Mol. Biol. 135*, 651–674.
Wishner, B. C., Hanson, J. C., Ringle, W. M., & Love, W. E. (1976) *Proc. Symp. Mol. Cell Aspects Sickle Cell Dis., DHEW Publ. (NIH) (U.S.) No. 76-1007*, 1–35.

Thermodynamics of Glycophorin in Phospholipid Bilayer Membranes†

A. Leo MacDonald and David A. Pink*

Theoretical Physics Institute, Center for Mathematical Simulation, St. Francis Xavier University, Antigonish, Nova Scotia, Canada B2G 1C0

Received May 1, 1986; Revised Manuscript Received September 17, 1986

ABSTRACT: We have developed a model of glycophorin in a phospholipid bilayer membrane in order to study the thermodynamics of this system and to understand the detailed behavior of recent calorimetric data. We assume that the larger glycophorin polar group can be considered as either adopting a pancakelike conformation at the bilayer interface (D state) or be directed generally away from the interface (U state) [Ruppel, D., Kapitza, H. G., Galla, H. J., Sixl, F., & Sackmann, E. (1982) *Biochim. Biophys. Acta 692*, 1–17]. Lipid hydrocarbon chains are described either as excited (e state) with high energy and relatively many gauche conformers or as generally extended (g state) with low energy. We performed a Monte-Carlo simulation using the Glauber and Kawasaki procedures on a triangular lattice which represents the plane of half of the bilayer. Lattice sites can be occupied either by lipid hydrocarbon chains or by model glycophorin α-helical hydrophobic cores. The states D and U are represented by hexagons of different sizes in the plane of the lattice, and the hard core repulsion between two such polar groups is accounted for by forbidding hexagon–hexagon overlap. We have studied the effect of having the glycophorin polar group interact in various ways with the lipid bilayer. We find that the protein polar group in its D state interacts, either directly or indirectly, with the lipid bilayer so as to reduce the effective lateral pressure acting on the lipid hydrocarbon chains by about 3 dyn/cm. Polar groups in their U states do not reduce this lateral pressure. We find that the region of reduced lateral pressure has a smaller area, in the plane of the bilayer, than the area of the region excluded by the protein polar group to penetration by other such polar groups, due to hard-core interactions. We find that as the protein concentration, c, increases from $c = 0$, the specific heat curves first broaden to a maximum at $c \approx c_1$ while the transition enthalpy decreases approximately linearly. At this concentration, the plane of the bilayer is essentially covered with protein polar groups in their D states. As c increases further, the specific heat curves narrow while the transition enthalpy stays approximately constant. As c increases still further, the specific heat peak broadens, and the transition enthalpy decreases. Our simulations show that this behavior is understood as a consequence of the bilayer behaving like a mixture of two kinds of lipids, one with the unperturbed lateral pressure acting on the chains and the other perturbed with a reduced lateral pressure acting on the chains. We calculate a phase diagram and show that it is remarkably similar to one deduced from measurements. Finally, we make predictions about the dependence of ^{2}H NMR line splitting upon protein concentration and propose experiments that may be performed to test predictions of the model.

A recent study of the effect of glycophorin upon the transition enthalpy of dimyristoylphosphatidylcholine (DMPC) bilayer membranes showed quite unexpected results (Ruppel et al., 1982), and there are indications that the concanavalin receptor in DMPC bilayers has a similar effect (Chicken & Sharom, 1984). It is possible that a similar effect may be associated with many glycoproteins, and it is our intention to present a theoretical model which, while it describes the behavior of glycophorin in DMPC, may have applications to glycoproteins in general.

There has been considerable interest in the interaction between membrane-spanning integral proteins and the phospholipids making up the quasi-two-dimensional lipid bilayer

†Supported by the Natural Sciences and Engineering Research Council of Canada.

0006-2960/87/0426-1909$01.50/0

membranes in which they are embedded (Chapman, 1982; Devaux & Seigneuret, 1985; Marsh & Watts, 1982; Hoffmann & Restall, 1984). Most of the studies have been concerned with proteins in which the portion of the protein inside the hydrophobic region of the membrane is as large as, or larger than, the portion within the water region. The effect of proteins such as rhodopsin or cytochrome oxidase upon the static properties of the lipid molecules is summarized by, e.g., Chapman (1982). In the case of sarcoplasmic reticulum ATPase, for example, the differential scanning calorimetry (DSC) peak gradually decreases in height and broadens though its maximum stays near the main lipid transition temperature (Gomez-Fernandez et al., 1980). The transition enthalpy data for sarcoplasmic reticulum ATPase in dipalmitoylphosphatidylcholine (DPPC) bilayer membranes (Gomez-Fernandez et al., 1980) display a monotonic decrease in ΔH as the protein concentration increases, with a constant slope. In the case of lipophilin (Boggs et al., 1980), ΔH decreases monotonically, as the lipophilin concentration increases, with increasing slope. These two kinds of behavior have been analyzed by Pink (1984) [see also Bach (1984)]. As the protein concentration increases, the steady-state fluorescence polarization, using a probe such as diphenylhexatriene (DPH), increases monotonically (Hoffmann et al., 1981; Chapman, 1982), as does the "immobile" components of the electron spin resonance (ESR) spectrum obtained by using nitroxide or similar spin-labels (Jost et al., 1973; Jost & Griffith, 1978; Silvius et al., 1984). The ^2H NMR spectrum shows that increasing protein concentration has little or no effect upon the static "order parameter" of the lipid hydrocarbon chains (Oldfield et al., 1978; Jacobs & Oldfield, 1981).

Some of these results have been analyzed in terms of a simple picture of such protein–lipid bilayers: The polar segments of integral proteins of this kind appear not to affect the state of the lipid hydrocarbon chains. These proteins have a slightly attractive effective interaction with those extended lipid hydrocarbon chains which are adjacent to the proteins, presumably because of the structure of the hydrophobic region of the proteins. However, because of the large number of lipid chain states with many gauche conformers ("excited" states) characteristic of lipids in a "fluid" phase, such integral proteins have excited lipid chains adjacent to them for temperatures greater than the main lipid phase transition temperatures, T_c, as well as for a range of temperatures below T_c, depending upon the protein concentration. Computer simulation calculations have resulted in a phase diagram (Lookman et al., 1982) which has been confirmed by the measurements of Davis (1983) on rhodopsin in DMPC [see also Lentz et al. (1985) for studies on the (Mg^{2+}–Ca^{2+})-ATPase of sarcoplasmic reticulum].

Glycophorin is ideally suited for studying the effects of an integral proteins' polar group on the lipid hydrocarbon chains. Most of the protein consists of a hydrophilic group attached to a much smaller hydrophobic α-helical segment which serves to orient the protein in the bilayer. Recent studies (Ruppel et al., 1982; Sackmann et al., 1984) involving glycophorin reconstituted in DMPC bilayer membranes showed that DSC curves displayed a quite different behavior from those obtained from the other protein–lipid systems described above. The DSC peak of the main lipid phase transition first broadens as the protein concentration increases from zero until $c = c_1$. It then sharpens as c is increased further through a narrow concentration range and then broadens again as the concentration is increased still further. The position of the maximum in the DSC curve first moves to a lower temperature as c increases to c_1 and then stays at a constant temperature while the sharpening occurs, before continuing to move again to lower temperatures at higher concentrations (Ruppel et al., 1982). The area under this peak, the transition enthalpy, decreased monotonically, as c increased, until $c = c_1$. At this concentration, it abruptly leveled off as c increased further through the narrow concentration range above and then decreased as the concentration increased still further. It is interesting to note that in the case of the concanavalin A receptor reconstituted in DMPC bilayer membranes, the transition enthalpy is reported to actually increase for $c > c_1$ (Chicken & Sharom, 1984).

Experiments involving energy transfer showed a complex behavior of energy-transfer rate with increasing c. These last results, however, enabled Ruppel et al. (1982) to propose the following behavior of glycophorin in DMPC bilayers: At very low concentrations, the large polar segment adopts a two-dimensional disk-like conformation on the surface of the bilayer, thus interacting with a large number of lipid molecules. This conformation is maintained by all glycophorin molecules until essentially the entire surface is so covered at $c = c_1$. Any further increase in c necessitates some of the polar segments adopting a more upright conformation, in that they project out of the plane of the bilayer, due to the packing with other proteins.

This proposal rationalized the results of the energy-transfer experiments. Furthermore, the characteristics of self-avoiding walks in two and three dimensions applied to the polar segment polymer suggested that it is indeed large enough to interact with the number of lipids deduced from the slope of the transition enthalpy as $c \rightarrow 0$. However, lacking any detailed calculations involving the transition enthalpy as a function of c, no explanation was given of the behavior of this quantity. In particular, it is not at all obvious why there is a sudden change in the slope of the transition enthalpy with c, followed by an essentially constant value of it with further increase in c.

Here we shall develop a Hamiltonian operator which describes a reasonable realization of the model outlined by Ruppel et al. (1982). We shall report the results of computer simulations applied to it and show that this model describes the detailed behavior of the DSC curves and the behavior of the transition enthalpy with c. Finally, we shall deduce a phase diagram from our simulations, compare it to the phase diagram proposed by Ruppel et al. (1982), and propose some experiments which could be carried out to see whether the model is correct.

The Model and the Simulation Procedure

There are three aspects to a model of glycophorin in a lipid bilayer membrane: (i) a model of a pure lipid bilayer in which the "main" phase transition is described; (ii) a model of glycophorin molecules in such a bilayer in which the conformational states of the polar segments and the interactions between the protein molecules are accounted for; (iii) a model which describes the interactions between glycophorin and lipid molecules.

(i) We shall make use of a lattice model previously used to study the thermodynamics of either pure lipid bilayers or bilayers containing certain integral proteins (Lookman et al., 1982; Pink, 1984). Each site of a triangular lattice (which represents the plane of one side of a lipid bilayer) can be occupied by a lipid hydrocarbon chain. This model assumes that each hydrocarbon chain can be in one of two states: a low-energy state representing a predominantly extended hydrocarbon chain and a high-energy state representing a chain that possesses a relatively large number of gauche bonds and

which is taken as "melted". The low-energy state is constructed from states which can be explictly listed and which contain, in addition to the all-trans state, states with jogs or one kink (Pink et al., 1980). Its construction has been described elsewhere (Pink, 1984) and involves a mean-field average over the states which go to make it up. It is important to recall, for use below, that the mean-field averaging which yields the low-energy state depends upon the local lateral pressure, Π, acting on the hydrocarbon chains, due to interactions in the polar region which brings the bilayer into existence (Marcelja, 1974; Georgallas et al., 1984).

The low-energy state, g, possesses internal energy, E_g, cross-sectional area, A_g, and degeneracy, D_g. The excited state, e, possesses internal energy, $E_e > E_g$, cross-sectional area, $A_e > A_g$, and degeneracy, $D_e >> D_g$. The Hamiltonian operator, from which all the thermodynamic functions of a pure lipid bilayer can be obtained, is

$$H_L = \frac{-J_0}{2}\sum_{\langle ij\rangle}\sum_{nm} I(nm)\ell_{in}\ell_{jm} + \sum_{in}\sum \epsilon_n \ell_{in} \qquad (1)$$

where ℓ_{in} is a lipid chain projection operator for state n (n = g, e) at lattice site i and I(nm) is the relative interaction [I(gg) = 1] between adjacent lipid chains in states n and m. J_0 is the strength of the interaction between two adjacent chains, both in state g, and $\langle ij\rangle$ denotes a summation over all sites i and over sites j which are nearest neighbors to i. $\epsilon_n = \Pi A_n + E_n - k_B T \ln D_n$, where Π is an effective lateral pressure, acting in the hydrophobic region of the bilayer, due to the interactions in the polar region which brings the bilayer into existence, k_B is Boltzmann's constant, and T is the absolute temperature. The numerical values given to the parameters have been described by Lookman et al. (1982).

(ii) In this paper, we are concerned with understanding the origins of the behavior of the DSC and heat of transition measurements of Ruppel et al. (1982), and we are not concerned with adjusting parameters to obtain merely good numerical agreement with experimental results. In order, therefore, to obtain good statistics for the results of our simulations, we shall represent glycophorin by a hypothetical "glycophorin" model. This possesses an "α-helical" core to which is attached a polar segment which, while it is large compared to a lipid chain, is smaller than the true size of glycophorin. Each model α helix occupies one site of the triangular lattice, and we assume that it undergoes no conformational changes. The large polar segment which is attached to an α helix can assume two predominant conformational states: the "down" state, D, where it takes on a pancakelike conformation, thus "covering" a relatively large number of lipid molecules, and the "up" state, U, which includes all conformations not contained in D, and which "covers" a relatively small number of lipid molecules. Since we are concerned only with the plane of the bilayer, we represent state D by a hexagon made up of R_D concentric hexagons (we refer to R_D as the "radius" of this hexagon), centered on the α-helix site, and which represents the projection of the polar segment pancake onto the plane of the bilayer. This state has internal energy E_D and degeneracy D_D. The state U is represented by a similar hexagon of "radius" R_U with internal energy E_U and degeneracy D_U. We choose $R_U < R_D$ and will discuss choices for the other parameters below. Because these hexagons represent polar group polymers, we require that hexagons associated with different proteins cannot interpenetrate or "overlap" each other due to the excluded volume repulsion or other interactions between the two polar segments. The Hamiltonian for the protein system alone is chosen to be

$$H_P = \frac{J_0}{2}\sum_{kk'}\sum_{aa'} H(|\vec{r}_a(k) - \vec{r}_{a'}(k')| - R_a - R_{a'} - 1)\rho_{ka}\rho_{k'a'} + \sum_k\sum_a \epsilon_a \rho_{ka} \qquad (2)$$

where $\vec{r}_a(k)$ is the position of the α helix of a protein located at site k when that protein has its polar segment in state a. ρ_{ka} is a projection operator for a protein with α helix located at site k and polar segment in state a. $H(x) = 0$ when $x > 0$, and $H(x) = \infty$ when $x < 0$. The first term of eq 2 thus ensures that two model glycophorin molecules cannot approach each other closer than the sum of the radii of their polar groups. The second term described the internal states of the polar groups with $\epsilon_a = E_a - k_B T \ln D_a$ where a = U or D. It seems plausible that the internal energies, E_U and E_D, due to bond rotation, when averaged over all conformations contributing either to state U or to state D, should be approximately equal. Accordingly, we have chosen $E_U = E_D = 0$. For the degeneracies, however, this cannot be the case. Hammersley et al. (1982) have shown that an unbranched freely jointed infinitely long polymer with one end anchored to a surface, treated as a self-avoiding walk, will project out of the plane of the surface (our U state) due to entropic effects. This means that $D_U >> D_D$. Our polar segment is of finite length and must represent a branched polymer. Accordingly, we have chosen D_U sufficiently greater than D_D to ensure that, in the absence of any other effects, it will be predominantly in state U. A choice of $D_U/D_D = 10$ achieved this.

(iii) The interaction between a model glycophorin and lipid molecules gives rise to two questions: How does the α helix interact with lipid hydrocarbon chains, and how does the model glycophorin polar group interact directly or indirectly with the lipid molecules? ^{2}H NMR measurements (Oldfield et al., 1978; Jacobs & Oldfield, 1981) have shown that the hydrophobic segments of a number of bilayer-spanning proteins induce little or no increase in the static "order parameter" of lipid hydrocarbon chains which are adjacent to them. This observation has been mathematically formulated and predictions made about the phase diagram of lipid bilayers containing such proteins (Lookman et al., 1982). The calculations are in accord with measurements (Bienvenue et al., 1982; Davis, 1983). Accordingly, we shall take over the results of Lookman et al. (1982) for the interactions between hydrocarbon chains and the α-helical core.

We shall assume that a large polar segment disrupts the forces in its neighborhood which bring the bilayer into existence. The effect of this is to reduce the effective lateral pressure, Π, acting on the lipid hydrocarbon chains which are "under" the polar segment in its D state. Such a change in Π will cause a change in A_g, E_g, and D_g, as well as the interactions I(g,n) and I(n,g). We should allow for the possibility that the region of the membrane surface which experiences the disruptive effect of the glycophorin polar group is not the same size as the region around a glycophorin α helix excluded to other proteins by the hard-core repulsion between glycophorin polar groups. This means that the region occupied by those lattice sites which experience the decreased effective lateral pressure is not the same size as the hexagonal regions, of "radii" R_U and R_D, which define the projection of the polar group on the surface. We define two hexagon radii R_{UP} and R_{DP} in units of concentric hexagons around an α-helix core site. Inside and on the boundary of these hexagons, lipid chain sites experience a decreased lateral pressure when the model protein is in an up or down state. Figure 1 shows a portion of a triangular lattice with model glycophorins in various states, together with the protein polar group's projected hard-core

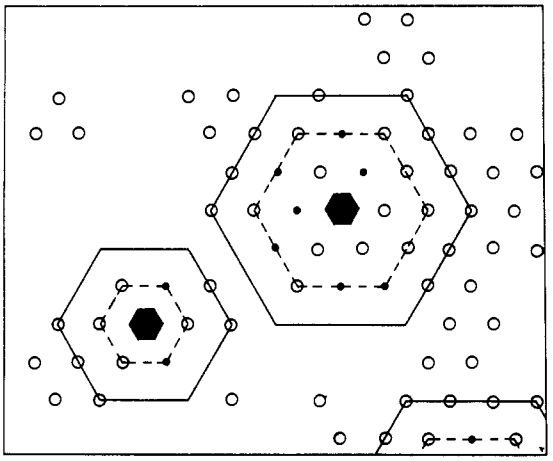

FIGURE 1: Example of one form of the model used. Solid black hexagons represent the α-helical cores. The regions on the perimeters of, and insde, the dashed hexagons are those of reduced pressure. The hexagons outlined by the solid lines represent the hard core due to the model protein's polar group. The large hexagons represent proteins in their down state while the small one represents one in its up state. The up protein cannot change to its down state because it is prevented by the hard core of the adjacent protein. The "radii" here are $R_U = 2$, $R_{UP} = 1$, $R_D = 3$, and $R_{DP} = 2$. Open circles represent lipid chains in their excited (or melted) state. Small filled circles represent chains in the reduced pressure region and in their low-energy (or extended) state. Unmarked sites represent chains outside of any reduced pressure region and in their extended state.

hexagon (of radii R_U and R_D) as well as the hexagons defining the regions of decreased lateral pressure (of radii R_{UP} and R_{DP}). Accordingly, the Hamiltonian describing the interaction of the proteins with the lipids is

$$H_{LP} = -J_0 \sum_{\langle ki \rangle} \sum_{n} K(n) \ell_{in} (\rho_{kU} + \rho_{kD}) + \sum_{k} \sum_{a} \rho_{ka} \left[\frac{-J_0}{2} \sum_{[ij]_{ka}} \sum_{nm} \Delta I_a(nm) \ell_{in} \ell_{jm} + \sum_{[i]_{ka}} \sum_{n} \Delta \epsilon_a(n) \ell_{in} \right] \quad (3)$$

Here, $K(n)$ represents the interaction between the α-helical core and an adjacent lipid chain in state n, and $\Delta I_a(n,m)$ is the change in the interaction between neighboring lipid chains in states n and m, when they are inside or on the boundary of the hexagon defining the region of decreased pressure when the protein is in state a. This hexagon is defined by R_{aP}. The set $[ij]_{ka}$ are those sites, i and j, which are nearest neighbors and which are inside or on the boundary or the decreased-pressure hexagon, or in the first lipid "layer" outside it, when the protein is in state a. The set of sites $[i]_{ka}$ are those which are inside or on the boundary of the decreased-pressure hexagon when the protein is in state a, and

$$\Delta \epsilon_a(n) = \Pi \Delta A_a(n) + \Delta \Pi_a A_n + \Delta \Pi_a \Delta A_a(n) + \Delta E_a(n) - k_B T \ln \{[D_n + \Delta D_a(n)]/D_n\} \quad (4)$$

$$H = H_L + H_P + H_{LP}$$

Here $\Delta \Pi_a$ is the change in lateral pressure for a chain affected by the decreased pressure hexagon of "radius" R_{aP}, when the protein is in state a. Similarly, $\Delta A_a(n)$, $\Delta E_a(n)$, and $\Delta D_a(n)$ are the changes in area, internal energy, and degeneracy of the lipid state n is this circumstance. All changes in the lipid parameters, ΔI_a, ΔA_a, ΔE_a, and ΔD_a, are completely determined once the value of $\Delta \Pi_a$ is given. The values of $K(n)$ were chosen so that the α-helical core alone, i.e., without any polar group, would leave the average area per chain unchanged as a function of core concentration for $T > T_c$ (Oldfield et al., 1978). If we choose $K(e) \approx 0$ on the grounds that the hydrophobic segment of an integral protein would interact only very weakly with an excited lipid chain, then the requirement above gives $K(g) \approx 0$. This says that integral proteins interact weakly with any lipid hydrocarbon chains adjacent to them so that the large number of excited states available ($D_e >> D_g$) dominates and ensures that hydrocarbon chains adjacent to proteins stay statically disordered down to some temperature below T_c [see Lookman et al. (1982) and Pink (1984)]. The choices for $\Delta \Pi_a$ will be described under Results.

A Monte-Carlo computer simulation procedure using the Glauber and Kawasaki realizations of the Metropolis algorithm (Metropolis et al., 1953; Binder & Stauffer, 1984; Pink, 1984) was used to study the thermodynamic behavior of the model. The plane of one side of the bilayer membrane was represented by an N by N triangular lattice with periodic boundary conditions. Each site of the lattice could be occupied either by an object representing a lipid hydrocarbon chain or by one representing the α-helical core of a protein. An α-helical core site served as the center of a hexagonal-shaped area of sites representing the projection, onto the plane of the membrane, of the hard core associated with the polar group of that α helix. It was also the center of a, possibly different, hexagonally shaped area of sites which, when occupied by lipid chains, experience a lateral pressure different from that experienced by lipids outside of such an area. In the Glauber change of state algorithm, lipids can attempt to change their state either from ground to excited or vice versa (g → e or e → g) while a protein can attempt to change its state from up to down or vice versa (U → D or D → U). The Kawasaki algorithm is used to try to change the position of a protein in the lattice by one lattice constant.

Typically, for a triangular lattice with $N = 40$, 100 Monte-Carlo steps were used to equilibrate the system, and 500 Monte-Carlo steps were used to measure the average values of thermodynamic functions. It was found that this number of steps was sufficient to obtain reliable averages for the quantities of interest.

RESULTS

Comparisons with Differential Scanning Calorimetry. The transition enthalpy, ΔH, of the model was calculated by measuring the area under the main peak of the specific heat curve. The method used to calculate this area is intended to mimic that used in practice. Generally, the base line is chosen such that only the area under the main peak in the DSC curves is used to determine ΔH of the main transition. In order, therefore, to compare the results of our model with experimental data, we have chosen a base line at $C_p = 0.4$ kcal mol^{-1} so as to obtain essentially all the area that can properly be associated with the DSC peak. This can be seen in Figures 3 and 5.

We investigated two different models of the protein in order to study the size of the excluded area due to the presence of the large polar segment, relative to the size of the area of reduced pressure "under" that polar group. In the first model (case I), the area of the reduced pressure around a protein is assumed greater than the hard-core excluded area ($R_{aP} > R_a$) while in the second (case II) the area of reduced pressure is smaller than the excluded area ($R_{aP} < R_a$). We also studied the cases in which the change in lateral pressure "under" an up protein polar group $\Delta \Pi_U$, either was equal to that "under" a down polar group, $\Delta \Pi_D$, or was zero. The justification for choosing $\Delta \Pi_U = 0$ is that if the polar segment is oriented away from the plane of the bilayer, then any perturbation of the

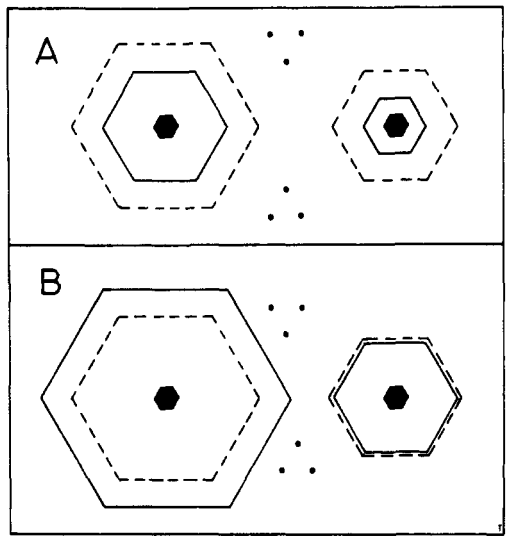

FIGURE 2: Solid hexagons represent α-helical cores. Dashed lines indicate the regions of reduced pressure while solid lines indicate the hard cores of the model protein's polar group. Small filled circles indicate the triangular lattice. (A) Case I: $R_U = 1$, $R_{UP} = 2$, $R_D = 2$, and $R_{DP} = 3$. (B) Case II: $R_U = 2$, $R_{UP} = 2$, $R_D = 4$, and $R_{DP} = 3$.

bilayer, due to it, should be small. The two cases studied were thus

case I: $R_U = 1$, $R_{UP} = 2$; $R_D = 2$, $R_{DP} = 3$ (Figure 2A)

case II: $R_U = 2$, $R_{UP} = 2$; $R_D = 4$, $R_{DP} = 3$ (Figure 2B)

both cases: $\Delta\Pi_U = \Delta\Pi_D$ or $\Delta\Pi_U = 0$

We found that the choice of $\Delta\Pi_U = \Delta\Pi_D$ did not give results in accord with experiment. This is not surprising: Unless there is some difference in the perturbation "under" an up and a down protein, we would expect to see a DSC peak with a monotonically increasing width, and a monotonically decreasing ΔH curve, as c increases. Accordingly, we shall not describe the results of these cases.

The results for cases I and II with $\Delta\Pi_U = 0$ and $\Delta\Pi_D = 3$ dyn/cm are shown in Figures 3–6. We found that we were not able to reproduce the shape of the ΔH vs. c curve unless $\Delta\Pi_D \approx 3$ or 4 dyn/cm. Figure 3 shows the calculated specific heat curves while Figure 4 shows ΔH and the fraction of model "glycophorin" molecules in their up state, f_U, for case I. The specific heat curves for case II are shown in Figure 5 while ΔH and f_U for that case are in Figure 6.

In order to understand the thermodynamic properties of the model bilayer, it should be realized that there are two kinds of lipids: those which are perturbed "under" a model "glycophorin" in its D state and so experience a reduced lateral pressure of ~27 dyn/cm ($\Delta\Pi_D = 3$ dyn/cm) and the unperturbed remainder which experiences a lateral pressure of 30 dyn/cm.

The results of case I are shown in Figures 3 and 4. It can be seen that the specific heat broadens until, at maximum broadening (D, E), about half of the lipids are perturbed so that there is approximately a 1:1 mixture of perturbed and unperturbed lipids. As c increases further, all lipids become perturbed so that a uniformly perturbed bilayer with a few α-helical "impurities" is achieved. This behaves like a nearly pure lipid bilayer, but with a reduced lateral pressure, and so the specific heat sharpens (G, H). The low "transition temperature" of ~13–15 °C shows that it is associated with

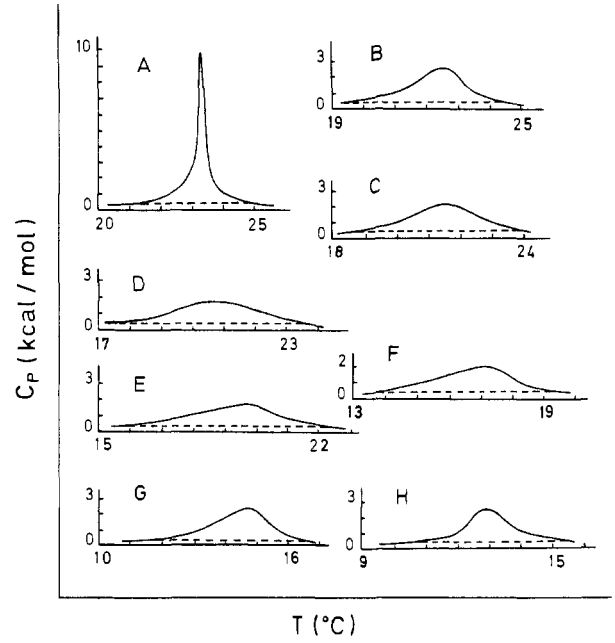

FIGURE 3: Computer simulation results for the specific heat, C_p, vs. temperature for different hexagon concentrations for case I. $\Delta\Pi_U = 0$ and $\Delta\Pi_D = 3$ dyn/cm. c is the mole fraction of hexagons. The dashed lines show the base line used, 0.4 kcal/mol, to calculate transition enthalpies. (A) $c = 0$; (B) $c = 0.00625$; (C) $c = 0.00938$; (D) $c = 0.0125$; (E) $c = 0.01875$; (F) $c = 0.03125$; (G) $c = 0.05$; (H) $c = 0.0625$.

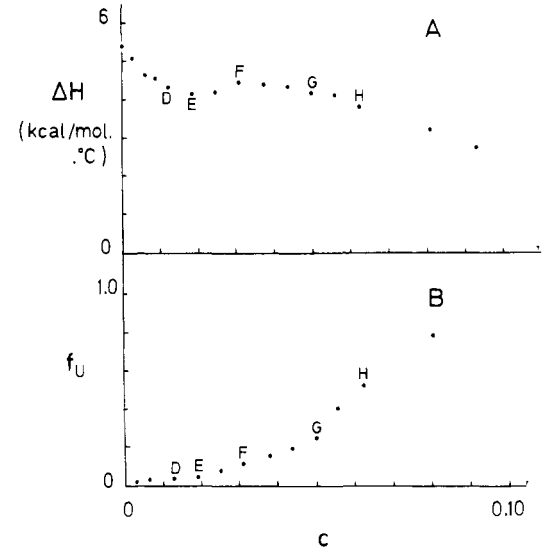

FIGURE 4: (A) Transition enthalpy for case I with $\Delta\Pi_U = 0$ and $\Delta\Pi_D = 3$ dyn/cm. (B) Fraction of hexagons in their up state, f_U, at $T = 18.2$ °C vs. hexagon concentration in mole fraction for case I with $\Delta\Pi_U = 0$ and $\Delta\Pi_D = 3$ dyn/cm. Points labeled D–H are associated with the corresponding specific heat curves of Figure 3.

perturbed lipids. Note that at concentration D, only about one half of the surface is covered by protein polar groups and that they are all in their down state.

Figures 5 and 6 show the results of case II. The specific heat peak broadens until this is a maximum at D. Note that f_U, the fraction of proteins in their U state, is equal to ~0.1, which is the same value as that at F in Figure 4B. Thus, at concentration D, essentially all of the surface is covered by protein polar groups in their down states, but only about half of the lipids are perturbed, which is why the specific heat peak is broadened maximally. As more proteins go into the "membrane", they can only be in their U state (though fluc-

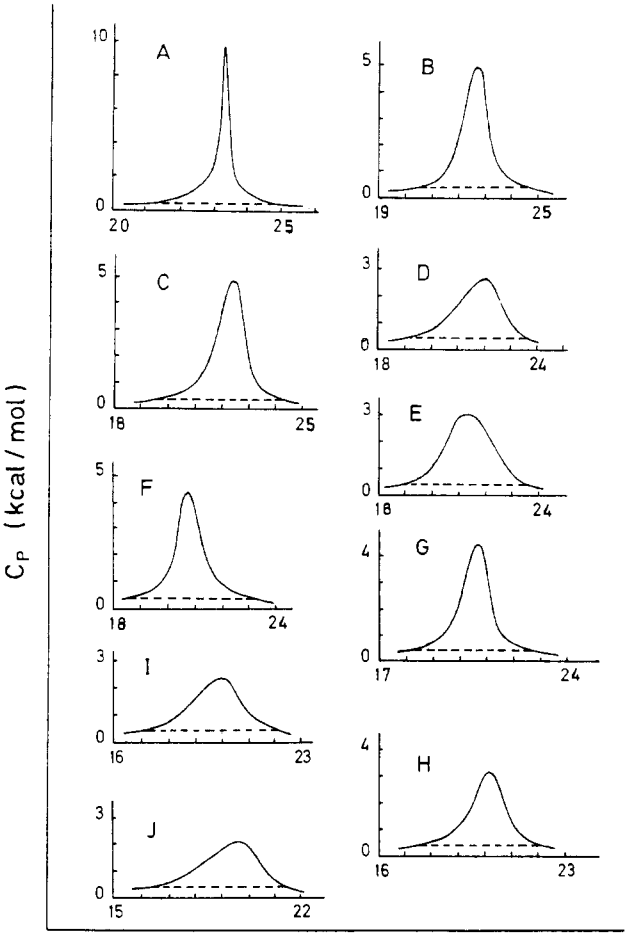

FIGURE 5: Computer simulation results for the specific heat, C_p, vs. temperature for different hexagon concentrations for case II. $\Delta\Pi_U = 0$ and $\Delta\Pi_D = 3$ dyn/cm. c is the mole fraction of hexagons. The dashed lines show the base line used, 0.4 kcal/mol, to calculate transition enthalpies. (A) $c = 0$; (B) $c = 0.0025$; (C) $c = 0.005$; (D) $c = 0.0075$; (E) $c = 0.01$; (F) $c = 0.0125$; (G) $c = 0.015625$; (H) $c = 0.021875$; (I) $c = 0.028125$; (J) $c = 0.0375$.

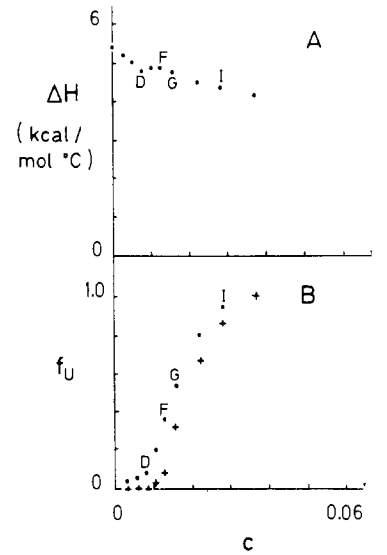

FIGURE 6: (A) Transition enthalpy for case II with $\Delta\Pi_U = 0$ and $\Delta\Pi_D = 3$ dyn/cm. (B) Fraction of hexagons in their up states, f_U, vs. hexagon concentrations in mole fraction for case II with $\Delta\Pi_U = 0$ and $\Delta\Pi_D = 3$ dyn/cm. $T = 18$ °C (●) and $T = 25.2$ °C (+). Points labeled D, F, G, and I are associated with the corresponding specific heat curves of Figure 5.

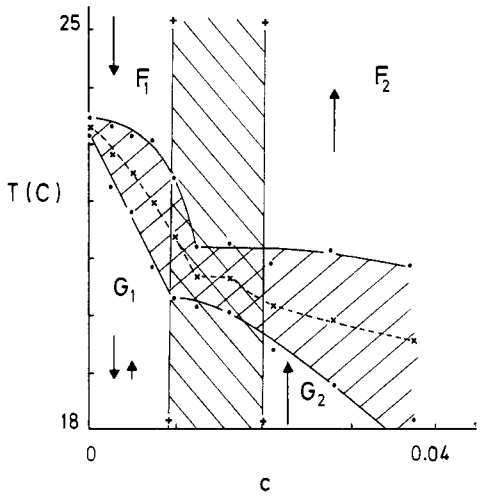

FIGURE 7: Phase diagram calculated from computer simulation results for case II with $\Delta\Pi_U = 0$ and $\Delta\Pi_D = 3$ dyn/cm. c is in units of mole fraction. The arrows indicate schematically the dominant state of the hexagons, up (↑) or down (↓). The near-vertical hatched area, in the region of $c \approx 0.01$–0.02, indicates a region where hexagon change of state occurs. Its boundaries (+) are the positions of the half-height of the derivatives of the two curves in Figure 6B. F_1 and F_2 indicate regions where the lipid chains are predominantly in their "fluid" or excited states, while G_1 and G_2 indicate regions where the chains are in their "gellike" or extended states. The dashed curve (×) is the locus of the peaks in the specific heat, C_p, of Figure 5. The closed circles, which define the limits of the second hatched region, indicate the positions of the half-heights of the specific heats of Figure 5. The solid lines drawn here are meant as a guide to the eye and should not be interpreted as phase boundaries.

tuations occur), so that f_U rises rapidly with c (F, G) and the fraction of unperturbed lipids increases from ~0.5. The lipids now behave like a mixture of lipids the great majority of which are unperturbed. The specific heat peak thus sharpens (F, G), and the "transition temperature" of ~21 °C shows that the lipids are predominantly unperturbed with $\Pi = 30$ dyn/cm. As even more proteins are added, the unperturbed lipids become diluted by α-helical core "impurities", and the specific heat peak broadens (I) with most of the proteins being in their U states ($f_U > 0.9$).

Comparing our results to the energy-transfer results of Ruppel et al. (1982), we see that case II, in which f_U begins to rise at concentration D (Figure 6) where ΔH levels off and the specific heat peak is broadest (Ruppel et al., 1982, Figures 3 and 4), describes the behavior of glycophorin. The point D locates the concentration $c = c_1$ referred to in the introduction.

Figure 7 shows the phase diagram deduced from the curves of Figure 5 and Figure 6B. The two nearly vertical lines are taken from Figure 6B: Smooth curves were drawn through the two sets of data points and differentiated with respect to concentration c. The concentrations at which the resulting peaks reached their half-height were plotted for each temperature, and the pairs of points near $c = 0.01$ and $c = 0.02$ were joined by straight lines. The resulting cross-hatched area defines the region where model glycophorin molecules are changing from a predominantly down state to a predominantly up state. From Figure 5, we calculated the temperatures at which various DSC curves had their maxima as well as their half-heights located for a given concentration. These points were connected and defined the second hatched area. The solid lines locate the temperatures of the half-heights while the dashed line locates the temperatures at which the specific heat has a maximum. The arrows indicate in a general way the conformations of the polar group in the regions shown. The protein polar groups are in their D states, at low concentration, despite the larger number of U states available ($D_U = 10D_D$)

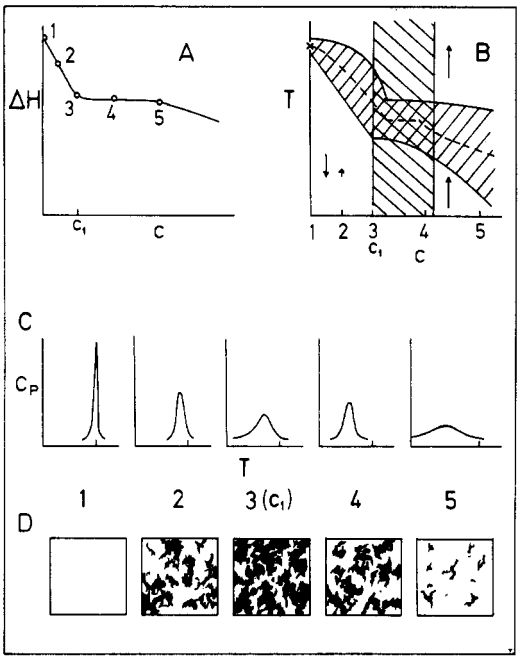

FIGURE 8: Schematic diagram relating the value or appearance of the transition enthalpy (A), the phase diagram (B), the specific heat (C), and the approximate area in the plane of the bilayer composed of perturbed lipid molecules under the glycophorin polar group in its D state (D), for five concentrations labeled 1–5. The concentration 3 is c_1. The fraction of the surface covered by protein polar groups in either of their two states is (1) 0, (2) ~0.5, and (3–5) 1.0. The fraction of these polar groups which are in their up state is (1–3) ~0, (4) ~0.5, and (5) ~1.0. The fraction of lipids which are perturbed is (1) 0, (2) ~0.3, (3) ~0.6, (4) ~0.3, and (5) ~0.

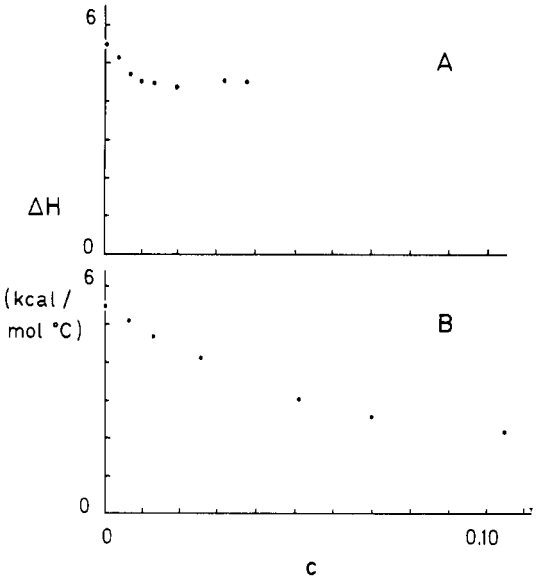

FIGURE 9: Computer simulation results for the transition enthalpy vs. hexagon concentration for case I. (A) All hexagons are constrained to be in their down states, and $\Delta\Pi_D$ = 3 dyn/cm. (B) All hexagons are constrained to be in their up states, and $\Delta\Pi_U$ = 0.

because the energy gained by coupling to the bilayer through the reduced pressure, $\Delta\Pi_D$, overcomes the entropy term which favors the U state. F_1, F_2, G_1, and G_2 denote two fluidlike and two gellike phases. A comparison between Figure 7 and Figure 5a of Sackmann et al. (1984) shows that their tentative phase diagram is remarkably similar to ours. Because our model glycophorin "molecules" are smaller, compared to the cross-section area of a melted lipid chain, than real glycophorin molecules, the numerical values of the concentrations in Figure 7 will be higher than the corresponding concentrations of Figure 5a (Sackmann et al., 1984) though the weight percents should be somewhat comparable. This difference is simply a matter of scaling and does not affect the conclusions drawn here. Figure 8 is a diagrammatic summary of our interpretation of the thermodynamics of glycophorin in DMPC bilayers. At five concentrations of particular significance, labeled 1–5, it relates ΔH to the phase diagram, shows the specific heat peaks at those concentrations, and shows schematically the fraction of lipids in the plane of the bilayer which are perturbed under glycophorin polar groups in their D states.

In order to understand why the two-state glycophorin model produces the correct shape for the ΔH vs. c curve, we performed the following simulation: The transition enthalpy as a function of glycophorin concentration was calculated for simulations where all the proteins were constrained to be in the down state. The area of reduced pressure for this down state was chosen to be larger than the excluded area ($R_{DP} > R_D$) in order that the effect be clearly seen, and the pressure reduction was $\Delta\Pi_D$ = 3 dyn/cm. A similar calculation was performed for the case where all proteins were pinned in the up state with $\Delta\Pi_U$ = 0. The results of ΔH are shown in Figure 9.

The ΔH vs. c curve, for the case when all the proteins were pinned in the up state, exhibits a continuous decrease with a changing slope. Since the pressure reduction for this up state was chosen to be zero, it is clear that this ΔH vs. c curve reflects only the effect of the α-helical protein core which simply acts as an impurity in the otherwise pure lipid matrix. This is in accord with the ΔH vs. c curve exhibited by many other intrinsic proteins such as lipophilin (Boggs et al., 1980) and described theoretically by Pink (1984).

The ΔH vs. c curve, for the case when all the proteins are pinned in the down state, however, exhibits a continuous decrease, with a steeper initial slope than in the "pinned-up" case, to a minimum value followed by a gradual *increase* up to a concentration which reflects maximum packing.

The explanation of this apparently peculiar behavior is easily understood when it is realized that what we have is a mixture of unperturbed lipids (Π = 30 dyn/cm) diluted by patches of perturbed lipids (Π = 27 dyn/cm). When c = 0, the pure unperturbed lipids melt at ~23.2 °C with $\Delta H \approx$ 5.5 kcal/mol. When the surface is essentially completely covered with "glycophorin" polar groups in their D state, however, all lipids are perturbed (recall that here $R_{DP} > R_D$; see Figure 2A) so that a specific heat peak characteristic of perturbed lipids slightly diluted with some α-helical "impurities" is observed. The transition temperature and transition enthalpy of this nearly pure system will be lower than those of the pure unperturbed case (see Figure 3H where that temperature is ~13 °C). When the unperturbed lipids are in the majority, the enthalpy lost from their transition (which is still the "main" transition) is hidden in the low-temperature wing of the specific heat and so not included in ΔH. Conversely, when the perturbed lipids are in the majority, enthalpy is lost from their transition (which is now the "main" transition) and is hidden in the high-temperature wing of the specific heat.

When half of the lipids are perturbed, the system is a 1:1 mixture of perturbed and unperturbed lipids, the specific heat is broadest (e.g., Figure 3D), and the transition enthalpy is a local minimum (Figure 9A, c = 0.02) since enthalpy is now hidden in both the high- and low-temperature wings.

Ruppel et al. (1982) calculated the number of lipids (N_L^U = 100 and N_L^D = 300) interacting with the up and down states, respectively, by extrapolating the high- and low-concentration

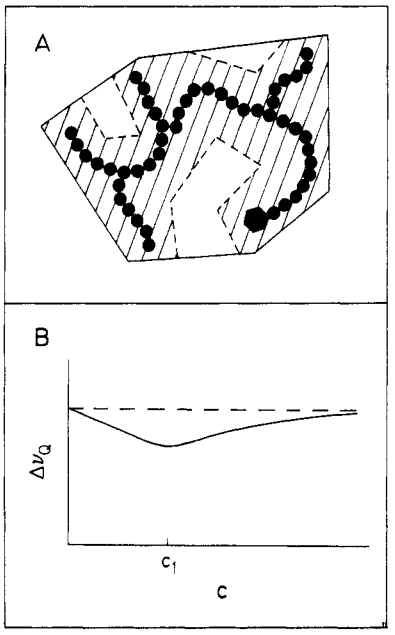

FIGURE 10: (A) Possible effect of a glycophorin polar group in a pancakelike conformation or down state, D. The area excluded to other glycophorin polar groups is shown by a solid line while the area of reduced pressure is indicated by the cross-hatched region. The large hexagon represents the end-on view of the α helix. The cross-hatched area is predicted to experience a reduced effective lateral pressure so that lipid hydrocarbon chains in that region are more disordered statically than chains elsewhere for $T > T_c$. (B) Qualitative predicted behavior of lipid hydrocarbon chain ^{2}H NMR line splitting, $\Delta\nu_Q$, as a function of glycophorin concentration for $T > T_c$. The concentration c_1, is the lowest concentration at which the ΔH vs. c curve levels off. This is seen in, for example, Figure 6A where $c_1 \approx 0.0125$ or in Figure 8 of Ruppel et al. (1982) where $c_1 \approx 0.0008$.

sections of the ΔH vs. c curve to zero. In the case of the determination of N_L^D, this procedure seems correct, and the extrapolated line by construction goes through the $c = 0$ value of ΔH (Ruppel et al., 1982; Figure 8). However, in the case of the determination of N_L^U, the extrapolated line does not go through the $c = 0$ value of ΔH, and therefore $N_L^U \approx 100$ may not be correct. It should also be pointed out that any determination of N_L^U from the high-concentration section of the ΔH vs. c curve might be suspect since it assumes that the low-concentration section of the ΔH vs. c curve has the same slope as the high-concentration section for the special case when all proteins are in their up state.

Discussion and Conclusions

Summary and Proposed Measurements on Glycophorin–Lipid Bilayer Membranes. We have presented a model of glycophorin in DMPC bilayer membranes and performed computer simulations to understand the measured dependence of thermodynamic quantities upon temperature and protein concentration. Our intention has been to understand quantitatively the results of DSC measurements in terms of a model which describes the large-scale conformational states of individual glycophorin molecules. We chose the model glycophorin to have a polar group 10–20 times smaller than that of a real glycophorin molecule in order to spend the computing time thereby gained on obtaining good statistics for thermodynamic functions. The differences in the concentrations between the results of Ruppel et al. (1982) and ours are thus merely a matter of scaling, though the weight percents of proteins reported by Sackmann et al. (1984) should be approximately comparable to those appropriate to our model. We chose our α helix to be represented by one lattice site which means that six lipid hydrocarbon chains could fit around it. The molecular dynamics simulation results of Edholm and Johansson (1987) indicate that the number is about seven or eight.

Following Ruppel et al. (1982), we assumed that the large-scale conformations of the larger glycophorin polar group could be described by two states, down and up, in which that polymer either adopted a pancakelike conformation near the plane of the bilayer or else did not. We have found that the experimental data can be understood if there is an effective interaction between the glycophorin polar group in its down state (pancake conformation) and the lipid molecules "underneath" it. This effective interaction could take the form either of a direct interaction between some of the components of the glycophorin polar segment and the polar groups of the lipid molecules, thereby tending to disrupt the bilayer and so disorder the hydrocarbon chains, or of an indirect interaction whereby the proximity of the glycophorin polar segment disturbs the water in the vicinity of the lipid polar groups, so weakening the forces which bring the bilayer into existence. The fact that we find that a weakening of those forces must occur means that the effective lateral pressure experienced by those lipid hydrocarbon chains under a polar group in its down state ($\Pi \approx 27$ dyn/cm) is less than the pressure on those lipid chains removed from such a perturbation ($\Pi = 30$ dyn/cm). We also find that the size of the area experiencing the reduced pressure under a down polar group is less than the excluded area, due to the hard-core repulsion, occupied by that polar group. This result might be made plausible by Figure 10A where it is seen that certain areas in the vicinity of the polar group of a protein may be excluded to penetration by the polar group of another protein yet not experience a weakened force.

We find that the model describes completely the protein concentration dependence of the DSC peak associated with the "main" lipid chain melting transition, as well as the associated unusual behavior of the transition enthalpy, ΔH. This is summarized in Figure 8. The unusual behavior of the DSC peak and ΔH is understood as the result of the bilayer being composed of a mixture of two kinds of lipids: perturbed lipids under part of a down glycophorin polar group and unperturbed lipids. As the protein concentration changes, the relative concentrations of these lipids change. The ΔH vs. c curve can be divided into three regions: (i) $0 < \eta < c_1$. The DSC peak broadens to a maximum, and ΔH decreases almost linearly. All proteins are in their D state. At c_1, essentially the entire membrane surface is "covered" by protein polar groups in their D state, but only about half of the lipids are perturbed. (ii) $c_1 < c$. The DSC peak narrows. The fraction of proteins in their up state increases rapidly toward unity. The entire surface of the membrane remains "covered" by protein polar groups, but the fraction of lipids which are perturbed decreases to zero. ΔH remains approximately constant with c because the system is in the cross-over region from "all-down" proteins to "all-up" proteins. (iii) $c_1 << c$. The number of α helices present becomes a significant amount of "impurities" so that the DSC peak broadens and ΔH decreases as c increases. Essentially all of the proteins are up, and most of the lipids have $\Pi = 30$ dyn/cm.

These results were summarized in Figures 7 and 8. The phase diagram (Figure 7) is remarkably similar to that of Sackmann et al. (1984). Because of the great difference in size of the model glycophorin used in the simulation and the real molecule, compared to the size of the lipid molecules, however, a direct comparison cannot be made between the results at equal concentrations.

Finally, if this model is correct, then we are able to make three predictions: (i) Some disturbance of the water layer in the lipid polar group region should be manifested for those regions of the phase diagram where the protein polar groups are predominantly in their pancakelike down state. This disturbance may be reflected in the order or dynamics of the lipid polar group and might be detected by NMR or other techniques. (ii) ^2H NMR spectra for $T > T_c$ might reflect the increased lipid hydrocarbon chain static disorder induced by the reduction in effective lateral pressure under a down protein's polar segment. Accordingly, $\Delta\nu_Q$ should first decrease and then increase as c increases from $c = 0$. This is shown qualitatively in Figure 10B where $c_1 \approx 0.0125$ for our model and $c_1 \approx 0.0008$ in the case studied by Ruppel et al. (1982). We have drawn $\Delta\nu_Q$ as returning to its $c = 0$ value as c increases beyong c_1. It is possible, however, that at high concentrations the values of $\Delta\nu_Q$ may lie above those values at $c = 0$. (iii) If it were possible to pin the polar groups of the proteins in either the up or the down states, then the predictions of Figure 9 could be checked. This might be possible by modifying the polar group of glycophorin, if necessary, so that each protein can act as a receptor to a molecule. They may then be able to be pinned in their up states. Alternatively, if lipids can be used which bind tightly to the protein polar groups, then they may be pinned in their down states. These two measurements would provide a value for N_L^U, the number of lipids interacting with an up protein, and the shape of ΔH vs. c for down proteins (Figure 9A), respectively.

All measurements should be carried out on glycophorin in sufficiently large unilamellar vesicles. The vesicles must be large enough so that the curvature of the vesicle plays a negligible part in the free energy. They must be unilamellar so that glycophorin polar groups do not interact with lipids belonging to bilayer sheets other than the one to which they are attached.

ACKNOWLEDGMENTS

We thank Erich Sackmann for his generosity in telling us his results, for his collaboration with us on glycoproteins, and for his most appreciated hospitality to D.A.P. in Munchen.

Registry No. DMPC, 13699-48-4.

REFERENCES

Bach, D. (1984) in *Biomembrane Structure and Function* (Chapman, D., Ed.) Vol. 4, pp 1–41, MacMillan Press, London.

Bienvenue, A., Bloom, M., Davis, J. H., & Devaux, P. G. (1982) *J. Biol. Chem. 257*, 3032–3038.

Binder, K., & Stauffer, D. (1984) in *Applications of the Monte Carlo Method in Statistical Physics* (Binder, K., Ed.) pp 1–36, Springer-Verlag, Heidelberg.

Boggs, J. M., Clement, I. R., & Moscarello, M. A. (1980) *Biochim. Biophys. Acta 601*, 134–151.

Chapman, D. (1982) *Biol. Membr. 4*, 179–229.

Chicken, C., & Sharom, F. (1984) *Biochim. Biophys. Acta 774*, 110–118.

Davis, J. H. (1983) *Biochim. Biophys. Acta 737*, 117–171.

Devaux, P. F., & Seigneuret, M. (1985) *Biochim. Biophys. Acta 822*, 63–126.

Edholm, O., & Johansson, J. (1987) *Eur. J. Biophys.* (in press).

Georgallas, A., Hunter, D. L., Lookman, T., Zuckerman, M. J., & Pink, D. A. (1984) *Eur. Biophys. J. 11*, 79–86.

Gomez-Fernandez, J. C., Goni, F. M., Bach, D., Restall, C., & Chapman, D. (1980) *Biochim. Biophys. Acta 598*, 502–516.

Hammersley, J. M. Torrie, G. M., & Whittington, S. G. (1982) *J. Phys. A: Math. Gen. 15*, 539–571.

Hoffman, W., & Restall, C. J. (1984) in *Biomembrane Structure and Function* (Chapman, D., Ed.) Vol. 4, pp 257–318, MacMillan Press, London.

Hoffman, W., Pink, D. A., Restall, C. J., & Chapman, D. (1981) *Eur. J. Biochem. 114*, 585–589.

Jacobs, R., & Oldfield, E. (1981) *Prog. Nucl. Magn. Reson. Spectrosc. 14*, 113–136.

Jost, P. C., & Griffith, O. H. (1978) in *Biomolecular Structure and Function* (Atris, P. F., Ed.) pp 25–54, Academic Press, New York.

Jost, P. C., Griffith, O. H., Capaldi, R. A., & Vanderkooi, G. (1973) *Proc. Natl. Acad. Sci. U.S.A. 70*, 480–484.

Lentz, B. R., Clubb, K. W., Alford, D. R., Hochli, M., & Meissner, G. (1985) *Biochemistry 24*, 433–442.

Lookman, T., Pink, D. A., Grundke, E. W., deVerteuil, F., Zuckermann, M. J. (1982) *Biochemistry 21*, 5593–5601.

Marčelja, S. (1974) *Biochim. Biophys. Acta 367*, 165–176.

Marsh, D., & Watts, A. (1982) in *Lipid–Protein Interactions* (Jost, P. C., & Griffith, O. H., Eds.) Vol. 2, pp 53–126, Wiley, New York.

Metropolis, N., Rosenbluth, A. W., Rosenbluth, M. N., Teller, A. H., & Teller, E. (1953) *J. Chem. Phys. 21*, 1087–1092.

Oldfield, E., Gilmore, R., Glaser, M., Gutowsky, H. S., Hshung, J. C., Kang, S. Y., King, T. E., Meadows, M., & Rice, D. (1978) *Proc. Natl. Acad. Sci. U.S.A. 75*, 4657–4660.

Pink, D. A. (1984) *Can. J. Biochem. Cell Biol. 62*, 760–777.

Pink, D. A. Green, T. J., & Chapman, D. (1980) *Biochemistry 19*, 349–356.

Ruppel, D., Kapitza, H. G., Galla, H. J., Sixl, F., & Sackmann, E. (1982) *Biochim. Biophys. Acta 692*, 1–17.

Sackmann, E., Kotulla, R., & Heiszler, F. J. (1984) *Can. J. Biochem. Cell Biol. 62*, 778–788.

Silvius, J. R., McMillen, D. A., Saley, N. D., Jost, P. C., Griffith, O. H. (1984) *Biochemistry 23*, 538–547.